Journal of Hazardous Materials 286 (2015) 484–492

Contents lists available at ScienceDirect

Journal of Hazardous Materials

journal homepage: www.elsevier.com/locate/jhazmat

$PM_{2.5}$ acidity at a background site in the Pearl River Delta region in fall-winter of 2007–2012

Xiaoxin Fu[a,b,c], Hai Guo[b,c,*], Xinming Wang[a,**], Xiang Ding[a], Quanfu He[a], Tengyu Liu[a], Zhou Zhang[a]

[a] Guangzhou Institute of Geochemistry, Chinese Academy of Sciences, China
[b] Department of Civil and Environmental Engineering, Hong Kong Polytechnic University, Hong Kong, China
[c] Shenzhen Research Institute, Hong Kong Polytechnic University, China

HIGHLIGHTS

- 24-h $PM_{2.5}$ samples were collected in fall-winter of 2007–2012.
- The annual reduction trends of $[H^+]_{total}$ and $[H^+]_{in\text{-}situ}$ of $PM_{2.5}$ was -32 ± 1.5 and -9 ± 1.7 nmol m^{-3}, respectively.
- On hazy days, the concentration of OM showed significant enhancement when $[H^+]_{in\text{-}situ}$ ranged from 85 to 240 nmol m^{-3}.
- $[H^+]_{in\text{-}situ}$ presented a close relationship with NO_3^- formation mechanisms in low and high acidity of $PM_{2.5}$.

ARTICLE INFO

Article history:
Received 21 September 2014
Received in revised form 5 January 2015
Accepted 6 January 2015

Keywords:
$PM_{2.5}$ acidity
Haze
Sulfate
Nitrate
Secondary organic carbon

ABSTRACT

Based on field observations and thermodynamic model simulation, the annual trend of $PM_{2.5}$ acidity and its characteristics on non-hazy and hazy days in fall-winter of 2007–2012 in the Pearl River Delta region were investigated. Total acidity ($[H^+]_{total}$) and in-situ acidity ($[H^+]_{in\text{-}situ}$) of $PM_{2.5}$ significantly decreased (*F*-test, $p < 0.05$) at a rate of -32 ± 1.5 nmol m^{-3} $year^{-1}$ and -9 ± 1.7 nmol m^{-3} $year^{-1}$, respectively. The variation of acidity was mainly caused by the change of the $PM_{2.5}$ component, i.e., the decreasing rates of $[H^+]_{total}$ and $[H^+]_{in\text{-}situ}$ due to the decrease of sulfate (SO_4^{2-}) exceeded the increasing rate caused by the growth of nitrate (NO_3^-). $[H^+]_{total}$, $[H^+]_{in\text{-}situ}$ and liquid water content on hazy days were 0.9–2.2, 1.2–3.5 and 2.0–3.0 times those on non-hazy days, respectively. On hazy days, the concentration of organic matter (OM) showed significant enhancement when $[H^+]_{in\text{-}situ}$ increased (*t*-test, $p < 0.05$), while this was not observed on non-hazy days. Moreover, when the acidity was low (i.e., $R = [NH_4^+]/(2 \times [SO_4^{2-}] + [NO_3^-]) > 0.6$), NH_4NO_3 was most likely formed via homogenous reaction. When the acidity was high ($R \leq 0.6$), the gas-phase formation of NH_4NO_3 was inhibited, and the proportion of NO_3^- produced via heterogeneous reaction of N_2O_5 became significant.

1. Introduction

Water soluble ions, organic matter (OM), and elemental carbon (EC) are main constituents of fine particle ($PM_{2.5}$) in the atmosphere [1–3]. The acidity of $PM_{2.5}$ is jointly determined by the amount of acidic components, i.e., sulfate (SO_4^{2-}) and nitrate (NO_3^-), and alkaline component, i.e., ammonium (NH_4^+) [4]. As an important indicator of particle properties, acidity is closely associated with human health, ecosystem, heterogeneous reaction of secondary aerosols, and hygroscopic property of aerosols [5–8].

Acidity influences the hygroscopic property of particles and subsequently changes the particle size distribution by affecting the liquid water content (LWC) [9–11], whereas the hygroscopicity and size distribution of particles greatly affect the optical property of aerosols [12–14]. Hence, visibility degradation such as haze closely links to aerosol acidity. Haze is defined as a weather phenomenon in which the daily mean visibility is less than 10 km, and the daily relative humidity (RH) is less than 90% [15]. Haze episode is usually characterized by the surge of secondary aerosols [16,17]. Although many laboratory studies show that acid-catalyzed heterogeneous reactions enhance the formation of secondary inorganic/organic aerosols [18–21], the relationship between aerosol acidity and secondary organic aerosols (SOA) in field measurements varies from site to site [22–26]. In particular, it is unclear how the aerosol acidity affects the SOA formation in highly polluted atmosphere such as the fast developing Pearl River Delta (PRD) region. Moreover, the correlations between aerosol acidity and SOA formation under different weather conditions such as hazy and non-hazy days remain unknown.

* Corresponding author at: Department of Civil and Environmental Engineering, Hong Kong Polytechnic University, Hong Kong, China. Tel.: +852 34003962; fax: +852 2334638.
** Corresponding author. Tel.: +86 2085290180; fax: +86 2085290706.
E-mail addresses: ceguohai@polyu.edu.hk (H. Guo), wangxm@gig.ac.cn (X. Wang).

http://dx.doi.org/10.1016/j.jhazmat.2015.01.022
0304-3894/

Fig. 1. The sampling site – Wanqingsha (WQS) and the surrounding environment.

Generally, the aerosol acidity is represented by two parameters, i.e., H^+_{total} and $H^+_{in\text{-}situ}$. H^+_{total} is the absolute acidity of aerosol, determined by total acids in aqueous extracts of filter samples. H^+_{total} is measured by two methods: (1) directly determining the pH of the aerosol extracts [27], and (2) calculating the difference between the concentrations of anions and cations (other than H^+) [28,29]. $H^+_{in\text{-}situ}$ is the actual acidity in the deliquesced aerosol, which influences the complex real-time reactions in atmospheric chemistry. H^+_{total} includes not only in-situ free hydrogen ion in the aerosol-phase, but also other hydrogen ions dissociated from bisulfate ions (HSO_4^-) by the large excess of water in aerosol aqueous extracts. Please note that due to low abundance of HCl and organic acids, their impact on $[H^+]_{total}$ was minor, and they were not included in the acidity calculation in this study [30–32]. Hence, H^+_{total} equals to the sum of $H^+_{in\text{-}situ}$ and HSO_4^- [33–35]. On the other hand, a number of thermodynamic models are developed to predict the $H^+_{in\text{-}situ}$, because direct measurement methods have not yet been established. The models for $H^+_{in\text{-}situ}$ include MARS [36], SCAPE2 [37], ISORROPIA [38] and Aerosol Inorganic Model (AIM-II) [39]. The AIM-II with the gas-aerosol partitioning calculation disabled is considered to be more accurate than others in calculating the aerosol acidity in earlier studies [34,40,41]. Although a number of field studies on aerosol acidity were carried out in recent years, all of them mainly focused on a certain period in a single year [33,35,40–46]. Limited field observation studies have been undertaken on the long-term variations of aerosol acidity in highly urbanized and polluted regions for successive years.

The PRD region in South China is one of the most economically dynamic areas in China, which occupies only 0.5% of the national land but contributes to ~10% of the national gross domestic products. High frequency of hazy days was often observed in the region in the past years. For instance, 144 hazy days were found in Guangzhou, the major city in the region, in 2004 [15]. Local government has implemented a series of control measures on the emission reduction from coal burning, motor vehicle exhaust, and industrial sectors, which resulted in the decrease of hazy days to ~70 days in 2012 (http://www.gzepb.gov.cn/). These control measures altered the emissions of airborne pollutants, leading to the change of chemical composition in $PM_{2.5}$ in these years. For instance, in fall-winter of 2007–2011, SO_4^{2-} and organic carbon (OC) in $PM_{2.5}$ reduced 1.7 and 1.1 $\mu g\,m^{-3}\,year^{-1}$, respectively, whereas NO_3^- increased 0.8 $\mu g\,m^{-3}\,year^{-1}$ [47]. Nevertheless, it is unclear how the acidic and alkaline components inevitably influence the aerosol acidity in these years. In this study, the annual trend of $PM_{2.5}$ acidity in the fall-winter of 2007–2012 in the PRD region was investigated in detail. The influence of $PM_{2.5}$ acidity on SOA on hazy and non-hazy days was compared.

2. Experimental

2.1. Site description

The sampling site, i.e., Wanqingsha (WQS; 22.42°N, 113.32°E), is a small town located near the center of the PRD (Fig. 1). The site is 50 km, 40 km, 50 km, and 25 km away from Guangzhou, Dongguan, Shengzhen, and Zhongshan, respectively. As a rural site, the local anthropogenic emissions are not significant because the surrounding area is farmland with very limited traffic and no coal-fired power plants and factories. The major air pollutants are mainly from the surrounding cities. As such, air masses arriving at this site were relatively aged, making it an ideal location to characterize the regional air pollution. The measurements were carried out on the rooftop of a 5-storey building (~30 m high).

2.2. Field sampling and chemical analysis

2.2.1. Field sampling

The field measurements focused on the most polluted fall-winter seasons. In the fall-winter season, the PRD region was generally influenced by the high-pressure ridges which made the weather cool and dry. Meanwhile, northeasterly monsoonal winds facilitated the accumulation of pollutants [48]. Hence, the high frequency of sunny days and stable meteorological conditions often caused severe air pollution over the PRD region [49,50]. In this study, 32, 29, 25, 53, 28 and 41 24-h $PM_{2.5}$ samples were collected in 2007, 2008, 2009, 2010, 2011 and 2012, respectively. The $PM_{2.5}$ samples were collected by drawing air through 8 × 10 in. quartz filters (QMA, Whatman, UK) using a high-volume sampler (Tisch Environmental Inc., Ohio, USA) at a rate of $1.1 \pm 0.04\,m^3\,min^{-1}$ for 24 h on selective days. Prior to field sampling, the quartz filters were pre-baked at 450 °C for 4 h, wrapped in aluminum foil, zipped in teflon bags, and stored at −20 °C. They were again stored in the same way after sampling. During the entire sampling periods, blank $PM_{2.5}$ samples were also collected every week. Visibility was detected using a Belfort Model 6000 visibility sensor (Belfort Instrument, USA). The meteorological parameters including wind speed/direction, temperature and relative humidity (RH) were measured by a mini weather station (Vantage Pro2™, Davis Instruments Corp., USA). The accuracy for RH was ±3% for the range of 0–90% RH, and ±4% for the range of 90–100% RH. The drift is ±0.5% per year. The resolution of temperature was 0.1 °C, and the accuracy was ±0.5 °C up to 43 °C. All the measured 1-min data of visibility, RH and temperature was averaged to the 24-h data according to the precise sampling hours.

2.2.2. Chemical analysis

After equilibrating the filter substrates to laboratory conditions, the $PM_{2.5}$ filters were weighed before and after field sampling at a temperature of 20–25 °C and a RH between 35 and 45%. For analysis of water-soluble inorganic ions, a punch (5.06 cm^2) of the filters was extracted twice with 10 mL ultrapure Milli-Q water and each for 15 min using an ultrasonic ice–water bath. The 20 mL water extracts were then filtered through a 0.22 μm pore size PTFE-filter (ANPEL Inc., Shanghai, China) and stored in a pre-cleaned HDPE bottle. The OC and EC in $PM_{2.5}$ were determined using an OC/EC analyzer (Sunset Laboratory Inc., USA) [51]. The cations (i.e., Na^+, NH_4^+, K^+, Mg^{2+} and Ca^{2+}) and anions (i.e., Cl^-, NO_3^-, and SO_4^{2-}) were analyzed with an ion-chromatography (Metrohm, 883 Basic IC plus). Cations were measured using a Metrohm Metrosep C4-100 column with 2 $mmol\,L^{-1}$ sulfuric acid as the eluent. Anions were measured using a Metrohm Metrosep A sup5-150 column with 3.2 $mmol\,L^{-1}$ Na_2CO_3 and 1.0 $mmol\,L^{-1}$ $NaHCO_3$ as the eluent. The method detection limits (MDLs) were 0.05, 0.01–0.05, and 0.02–0.03 $\mu g\,m^{-3}$ for OC/EC, cations, and anions, respectively.

2.2.3. Quality assurance/quality control (QA/QC)

During the sampling periods, the flow rate of the $PM_{2.5}$ sampler was monthly calibrated by using a manometer (Thermo, USA) to monitor the pressure differential across the filter. The standard procedure in the manufacturer's handbook was strictly followed to obtain the required flow rate. After the calibration, the actual flow rate of the sampler ranged from 1.05 to 1.17 $m^3\,min^{-1}$ with an average value of $1.11 \pm 0.04\,m^3\,min^{-1}$.

Field and laboratory blank samples were analyzed in the same way as field samples. All the OC/EC and cation/anion data were corrected using the field blanks. The average concentrations in blank samples for Na^+, NH_4^+, K^+, Mg^{2+}, Ca^{2+}, Cl^-, NO_3^- and SO_4^{2-}

were 0.03 ± 0.01, 0.00 ± 0.01, 0.02 ± 0.01, 0.02 ± 0.01 0.02 ± 0.01, 0.03 ± 0.01, 0.05 ± 0.02, 0.04 ± 0.02 ppm, respectively, while the average values of OC and EC in the blank filter were 0.29 ± 0.22, 0.00 ± 0.21 $\mu gC\,cm^{-2}$, respectively.

Methane was used as the internal standard to quantify the concentrations of OC and EC. Glucose solution with concentration gradients of 0.427, 4.289 and 128.19 $\mu g\,\mu L^{-1}$ was weekly used as the external standards to test the linear stability of the instrument. The correlation coefficient was $99.9 \pm 0.3\%$, and the relative standard deviation was 1.72%.

2.3. Calculation of PM_5 acidity

2.3.1. Total acidity

The ratio of nano-mole concentration (nmol m^{-3}) of NH_4^+ to SO_4^{2-} and NO_3^- was used to indicate the acidic property of $PM_{2.5}$.

$$R = [NH_4^+]/(2 \times [SO_4^{2-}] + [NO_3^-] \quad (1)$$

In this equation, $R \leq 1$ indicates that the aerosol is acidic, while $R > 1$ means that most of acids are neutralized by NH_4^+. Total acidity was calculated using the following equation:

$$[H^+]_{total} = 2 \times [SO_4^{2-}] + [NO_3^-] - [NH_4^+] \quad (2)$$

$[H^+]_{total} < 0$ indicated that the aerosol solution was alkaline, and the samples with $[H^+]_{total} < 0$ did not involve in the next model calculation of $[H^+]_{in\text{-}situ}$. In this study, SO_4^{2-}, NO_3^- and NH_4^+ were the key factors to determine the aerosol acidity, and they contributed to about 90% of the mass of total ionic species. The low abundance of other ions (i.e., Na^+, K^+, Cl^-, Ca^{2+} and Mg^{2+}) suggested that they had weak influence on the aerosol acidity. In addition, the concentrations of water-soluble organic acids constituted only about 1–4% of the total ions, indicating negligible impact on the acidity estimated by H_2SO_4 and HNO_3 [30,31].

2.3.2. In-situ acidity and pH

In-situ aerosol acidity was calculated by AIM-II model $H^+ - NO_3^- - SO_4^{2-} - NH_4^+ - H_2O$ with gas-aerosol partitioning disabled (http://www.aim.env.uea.ac.uk/aim/model2/model2a.php). The 24-h averaged temperature, RH, $[SO_4^{2-}]$, $[NO_3^-]$, $[NH_4^+]$ and $[H^+]_{total}$ were input into the model. Please note, due to the fact that exchange between alkaline group and target ions in ion chromatography (IC) caused both H_2SO_4 and HSO_4^- to be SO_4^{2-}, the concentration of HSO_4^- reported in this study was not measured by the instrument (i.e., IC) but estimated by the AIM-II model. The AIM-II is a state-of-art model which can estimate aerosol acidity, and liquid-phase and solid-phase ionic components in the in-situ aerosols at variable temperature and RH [39]. Although other models such as SCAPE and ISORROPIA take into account more ion species than SO_4^{2-}, NO_3^- and NH_4^+, they cannot be used in the present study because the required gas-phase concentrations of HNO_3, HCl and NH_3 were unavailable. In addition, there are 3 other versions of AIM model, i.e., AIM-I, AIM-III and AIM-IV. AIM-I model was not suitable because Br^- was under the detection limit during the whole sampling periods. AIM-III includes Na^+ and Cl^- in the calculation system and only allows modeling at a fixed temperature of 298.15 K. However, the mass concentrations of Na^+ and Cl^- only constituted $6.5 \pm 0.5\%$ of the total water-soluble species in this study. Moreover, the 24-h-averaged temperature fluctuated between 278.7 K and 300.5 K. Therefore, AIM-III model was not appropriate. AIM-IV only allows modeling at RH > 60%, while the average RH was 43.6% in 2008 in this study. Hence, the AIM-IV model was also unsuitable. Among the total 208 samples, 11 completely-neutralized particles (i.e., $[H^+]_{total} < 0$) and 8 un-deliquescence particles (i.e., LWC = 0) were excluded for the analysis of $H^+_{in\text{-}situ}$ and pH.

The in-situ pH of aerosol is calculated using the following equation:

$$pH = -\log(\gamma \times [H^+]_{in\text{-}situ} \times \rho/m \quad (3)$$

where γ is the activity coefficient of $H^+_{in\text{-}situ}$. It was variable for different $H^+_{in\text{-}situ}$ estimated for different samples. The average value of the activity coefficient of $[H^+]_{in\text{-}situ}$ was 6.1 ± 1.7 during the entire sampling period. $[H^+]_{in\text{-}situ}$ is the concentration of $H^+_{in\text{-}situ}$ in nanomole per cubic meter, ρ is the density of $(NH_4)_2SO_4$ in gram per cubic centimeter calculated by empirical equations [52], and m is the sum of LWC and the total water-soluble inorganic ions in mass concentration with the unit of microgram per cubic meter.

3. Results and discussion

3.1. Annual trends of aerosol acidity

In fall-winter of 2007–2012, all of the measured samples with both negative and positive values were used to reveal the actual variation of $[H^+]_{total}$. $[H^+]_{total}$ ranged from −43 to 480 nmol m^{-3}, with an average of 123 ± 13 nmol m^{-3} (average ±95% confidence

Table 1
Concentrations of $[H^+]_{total}$, $[H^+]_{in\text{-}situ}$ and LWC, pH and meteorological data in fall-winter of 2007–2012 (average ± 95% confidence interval).

Year	Period	$[H^+]_{total}$ (nmol m^{-3})	$[H^+]_{in\text{-}situ}$ (nmol m^{-3})	$[HSO_4^-]$(nmol m^{-3})	pH	LWC ($\mu g\,m^{-3}$)	T (°C)	RH (%)
2007	Haze	257 ± 111	82 ± 54	175 ± 59	−0.04 ± 0.37	54 ± 15	23.6 ± 1.0	75.6 ± 2.4
	Non-haze	198 ± 35	48 ± 17	144 ± 22	−0.37 ± 0.24	27 ± 6	22.2 ± 0.9	66.0 ± 4.0
	Average	211 ± 37	55 ± 18	151 ± 21	−0.30 ± 0.21	33 ± 7	22.5 ± 0.8	68.1 ± 3.4
2008	Haze	325 ± 134	127 ± 127	177 ± 58	−0.97 ± 0.92	23 ± 9	17.8 ± 3.2	52.4 ± 8.3
	Non-haze	148 ± 17	36 ± 13	88 ± 16	−1.13 ± 0.33	8 ± 2	17.7 ± 1.1	42.6 ± 4.5
	Average	166 ± 28	47 ± 19	99 ± 18	−1.11 ± 0.29	9 ± 3	17.7 ± 1.1	43.6 ± 4.3
2009	Haze	140 ± 31	40 ± 11	99 ± 23	0.07 ± 0.19	47 ± 13	19.5 ± 0.9	77.5 ± 4.1
	Non-haze	151 ± 22	21 ± 5	109 ± 24	−0.34 ± 0.28	20 ± 7	15.2 ± 1.5	59.1 ± 6.2
	Average	146 ± 18	30 ± 7	104 ± 17	−0.15 ± 0.20	32 ± 9	17.1 ± 1.3	67.2 ± 5.3
2010	Haze	182 ± 86	77 ± 51	113 ± 40	0.33 ± 0.50	64 ± 31	19.4 ± 1.0	74.0 ± 4.8
	Non-haze	95 ± 23	26 ± 11	57 ± 16	0.47 ± 0.32	20 ± 4	20.1 ± 1.3	68.7 ± 3.2
	Average	116 ± 30	39 ± 17	71 ± 17	0.47 ± 0.27	32 ± 10	19.9 ± 1.0	70.5 ± 2.8
2011	Haze	87 ± 28	16 ± 8	72 ± 22	0.88 ± 0.31	49 ± 8	23.3 ± 1.6	78.1 ± 2.4
	Non-haze	82 ± 8	13 ± 3	63 ± 10	0.31 ± 0.23	25 ± 7	19.5 ± 1.6	69.0 ± 4.3
	Average	83 ± 8	13 ± 3	65 ± 9	0.42 ± 0.21	30 ± 7	20.2 ± 1.5	70.7 ± 3.7
2012	Haze	97 ± 67	26 ± 22	71 ± 46	0.77 ± 0.43	71 ± 21	22.6 ± 0.8	83.8 ± 3.4
	Non-haze	58 ± 14	11 ± 2	49 ± 11	0.73 ± 0.22	29 ± 4	21.3 ± 1.2	80.0 ± 3.0
	Average	43 ± 16	13 ± 4	51 ± 12	0.81 ± 0.24	45 ± 22	20.4 ± 1.1	84.9 ± 3.2

interval). During the 6-year sampling period, the ratio between $[NH_4^+]$ and $[SO_4^{2-}]$ was 2.2 ± 0.1; so the liquid phase of aerosol could be treated as the solution of $(NH_4)_2SO_4$. In addition, the estimated ρ for the aerosol solution ranged from 1.21 to 1.25 g cm^{-3}. Hence, the calculated $[H^+]_{in\text{-}situ}$ changed from 0.2 to 240 nmol m^{-3}, with an average of 34 ± 6 nmol m^{-3}. As shown in Table 1 and Fig. 2, $[H^+]_{total}$ ($R^2 = 0.99$) and $[H^+]_{in\text{-}situ}$ ($R^2 = 0.86$) significantly decreased (F-test, $p < 0.05$) at a rate of -32 ± 1.5 nmol m^{-3} year^{-1} (or -27% year^{-1}) and -9 ± 1.7 nmol m^{-3} year^{-1} (or -25% year^{-1}), respectively. In contrast, pH showed an increasing rate of 0.3 ± 0.1 year^{-1} or 22% year^{-1} in these years ($R^2 = 0.69$, F-test, $p < 0.05$).

The decreasing trends of $[H^+]_{total}$ and $[H^+]_{in\text{-}situ}$ were likely caused by the following reason. Our previous study reported that $[SO_4^{2-}]$ reduced at a rate of 18 nmol m^{-3} year^{-1} and $[NO_3^-]$ presented a growth trend with a rate of 13 nmol m^{-3} year^{-1}, while $[NH_4^+]$ was relatively stable at the same site in fall-winter of 2007–2011 [47]. According to stoichiometry, the H^+_{total} provided by SO_4^{2-} was twice than that provided by NO_3^- in an excessive amount of water extracts of aerosol. In addition, SO_4^{2-} accounted for $19 \pm 1\%$ of the $PM_{2.5}$ mass, about twice the percentage of NO_3^- ($10 \pm 1\%$). Together, the decreasing rate of $[H^+]_{total}$ due to the decrease of $[SO_4^{2-}]$ exceeded the increasing rate of $[H^+]_{total}$ caused by the growth of $[NO_3^-]$ in these years. Furthermore, it was found that pH value was the lowest in 2008 because the concentrations of LWC and aerosol aqueous solution were the lowest in this year. Correlation analysis indicated that the lowest LWC concentration in 2008 corresponded to the lowest average RH ($44 \pm 4\%$) (Table 1), suggesting the close relationship between LWC and RH, consistent with previous studies [33,41,53].

High aerosol acidity usually appeared on the day when there was large difference in concentration between acidic and alkaline components of $PM_{2.5}$. For instance, $[H^+]_{total}$ soared to 480 nmol m^{-3} on October 27, 2007, and $[H^+]_{in\text{-}situ}$ reached as high as 240 nmol m^{-3} on December 20, 2012. It was noteworthy that the days with low $[H^+]_{in\text{-}situ}$ were not always clean, because the amount of $[H^+]$ was influenced by LWC which dissociated H^+ from solid-acid in aerosol. For instance, on December 7, 2010, $[H^+]_{in\text{-}situ}$ was only 4 nmol m^{-3}, while $[SO_4^{2-}]$, $[NO_3^-]$ and $[NH_4^+]$ reached as high as 353.6, 204.7 and 734.2 nmol m^{-3}, respectively. Note that the RH was only 56%, and the mass concentration of LWC was only 6 μg m^{-3} on that day, suggesting that low LWC concentration was not conducive to the dissociation of $H^+_{in\text{-}situ}$.

By comparison, the annual average levels of aerosol acidity in this study were higher than those in previous studies conducted in the region, in which $[H^+]_{total}$ was about 90 nmol m^{-3}, and $[H^+]_{in\text{-}situ}$ ranged from 6 to 20 nmol m^{-3} [45,46]. Note that apart from the levels of chemical component in $PM_{2.5}$, different aerosol acidity obtained in different studies was also related to the different sampling sites, sampling periods and sampling methods, i.e., sampler with denuder versus on-line monitoring equipment.

3.2. $[H^+]_{in\text{-}situ}$ and PM_5 chemical components in hazy and non-hazy periods

3.2.1. Aerosol acidity

The $[H^+]_{total}$, $[H^+]_{in\text{-}situ}$, $[HSO_4^-]$, LWC, pH, temperature and RH in hazy and non-hazy periods during fall-winter of 2007–2012 are listed in Table 1. The annual trends of $[H^+]_{total}$, $[H^+]_{in\text{-}situ}$ and $[HSO_4^-]$ on non-hazy and hazy days are shown in Figs. 3 and 4, respectively. Overall, there were 153 non-hazy days and 44 hazy days. Eleven samples with RH > 90% and visibility < 10 km were excluded from the non-hazy days and from data analysis.

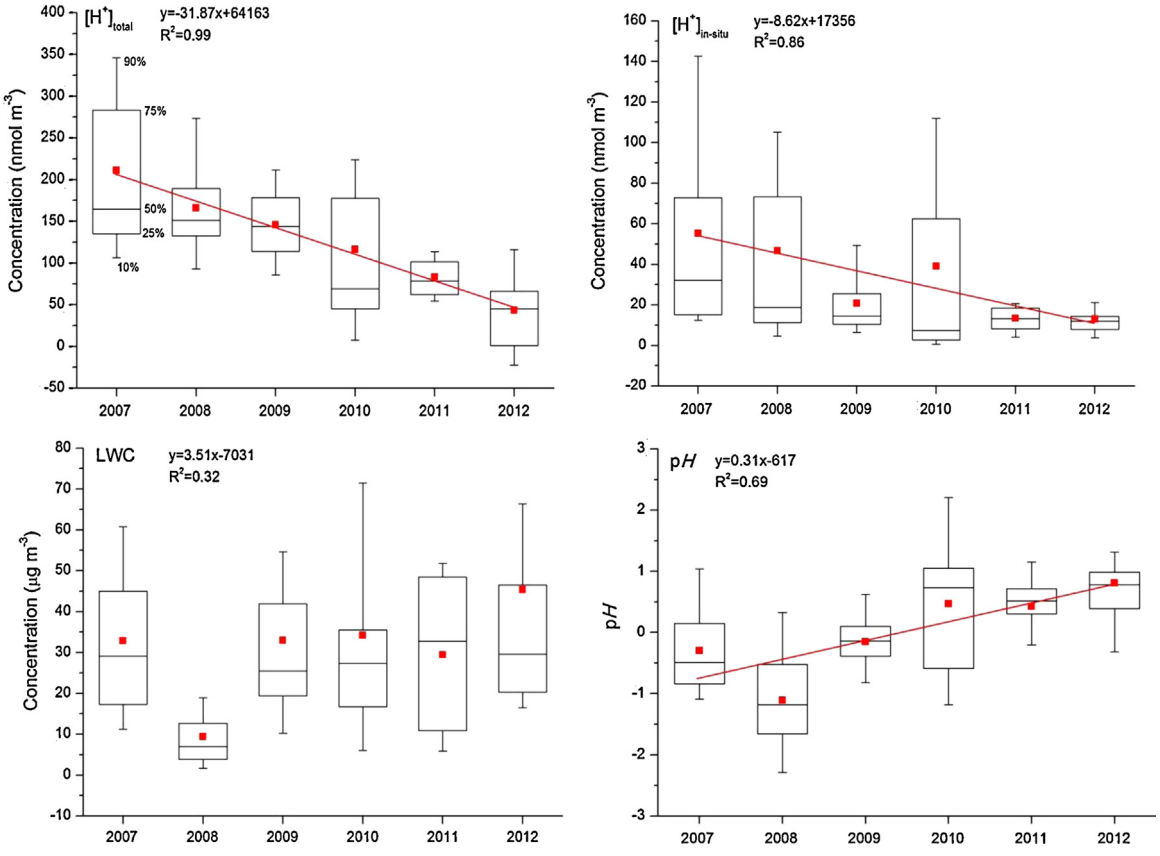

Fig. 2. Annual variations of $[H^+]_{total}$, $[H^+]_{in\text{-}situ}$, LWC and pH in fall-winter from 2007 to 2012.

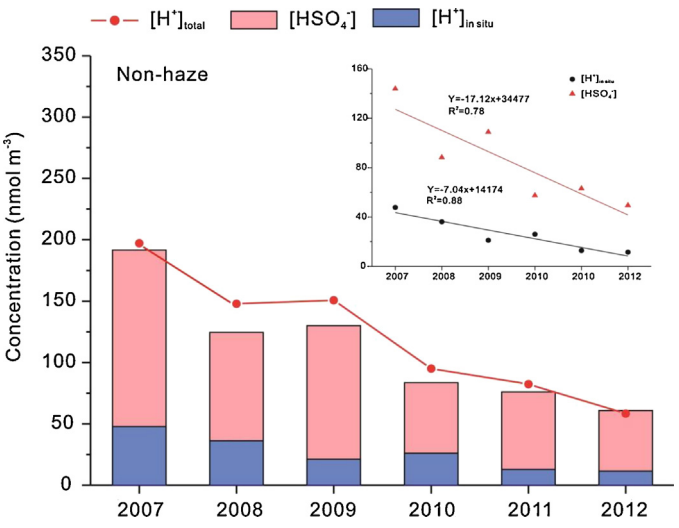

Fig. 3. Annual trends of $[H^+]_{total}$, $[H^+]_{in\text{-}situ}$ and $[HSO_4^-]$ on non-hazy days during in fall-winter of 2007–2012.

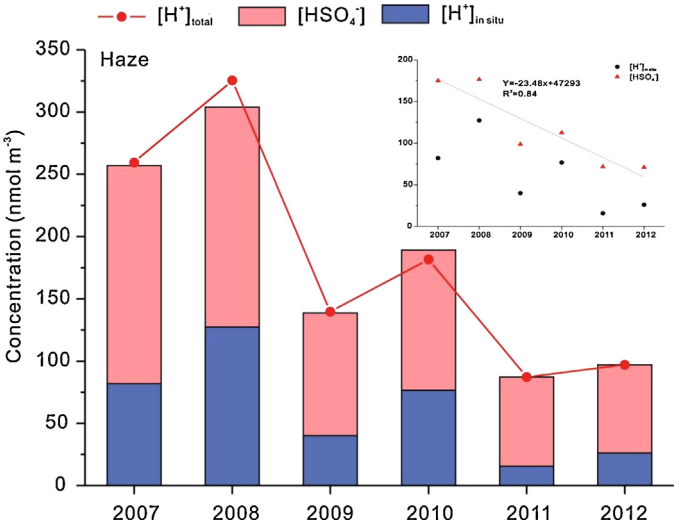

Fig. 4. Annual trends of $[H^+]_{total}$, $[H^+]_{in\text{-}situ}$ and $[HSO_4^-]$ on hazy days during in fall-winter of 2007–2012

During non-hazy period, the yearly average $[H^+]_{in\text{-}situ}$ and $[HSO_4^-]$ were highest in 2007 and lowest in 2012. Both $[H^+]_{in\text{-}situ}$ and $[HSO_4^-]$ significantly decreased at a slope of -7 ± 1.3 and -17 ± 4.5 nmol m^{-3} year^{-1}, respectively (F-test, $p < 0.05$). The average percentage of $[H^+]_{in\text{-}situ}$ and $[HSO_4^-]$ in $[H^+]_{total}$ was $19 \pm 4\%$ and $71 \pm 7\%$, respectively. In hazy period, the yearly average $[H^+]_{in\text{-}situ}$ and $[HSO_4^-]$ were highest in 2008 and lowest in 2011. $[HSO_4^-]$ decreased at a rate of -24 ± 5.1 nmol m^{-3} year^{-1} (F-test, $p < 0.05$), while $[H^+]_{in\text{-}situ}$ did not show obvious decreasing trend (F-test, $p = 0.1$) perhaps due to the supplementary effect of secondarily formed organic/inorganic acids. Moreover, on hazy days the average percentage of $[H^+]_{in\text{-}situ}$ and $[HSO_4^-]$ in $[H^+]_{total}$ reached $27 \pm 11\%$ and $71 \pm 8\%$, respectively. By comparison, the $[H^+]_{total}$, $[H^+]_{in\text{-}situ}$, $[HSO_4^-]$ and LWC on hazy days were 0.9–2.2, 1.2–3.5, 0.9–2.0 and 2.0–3.0 times than those on non-hazy days, respectively. Due to combined impact of $[H^+]_{in\text{-}situ}$, activity coefficient of $H^+_{in\text{-}situ}$ and mass concentration of aerosol solution, the average pH values on non-hazy days were lower than those on hazy days, except for 2010. The inverse pattern of pH in 2010 might be due to the similar value of activity coefficient of $H^+_{in\text{-}situ}$ in both non-hazy and hazy periods, which was 2.7 and 2.2 (t-test, $p > 0.05$), respectively.

It is noteworthy that the proportion of $[HSO_4^-]$ in $[H^+]_{total}$ was similar during both the hazy and non-hazy periods, while the percentage of $[H^+]_{in\text{-}situ}$ in $[H^+]_{total}$ was higher on hazy days than that on non-hazy days. That is, the influence of abundant LWC which generally appeared in hazy periods did not decrease the molarity of in-situ solution, but generated more dissociated in-situ H^+. The similar proportion of $[HSO_4^-]$ in $[H^+]_{total}$ during both hazy and non-hazy periods revealed that the excess $[H^+]_{in\text{-}situ}$ in hazy periods was not caused by the dissociation of HSO_4^-, but probably by the secondarily formed water-soluble organic/inorganic acids. In addition, the increase was also the main reason for insignificant decreasing trend of $[H^+]_{in\text{-}situ}$ in hazy periods. On the other hand, the unexplained part of $[H^+]_{total}$ on non-hazy days in 2008–2010 (Fig. 3) was likely due to the relatively low concentrations of LWC, which could not completely deliquesce in-situ aerosols, resulting in part of H^+_{total} existing in solid phase. Compared to previous studies, the $[H^+]_{total}$ and $[H^+]_{in\text{-}situ}$ values on hazy days of 2007 and 2008 in this study were higher than those obtained in Jinan, North China [44], and in Hong Kong, South China [46].

3.2.2. Relationship between $H^+_{in\text{-}situ}$ and chemical composition of PM_5

Fig. 5 shows the chemical composition of $PM_{2.5}$ with low and high in-situ acidity which was differentiated by the threshold of $[H^+]_{in\text{-}situ} = 83$ nmol m^{-3} (i.e., $R = 0.6$ as discussed in Section 3.3) during non-hazy and hazy periods. On non-hazy days, the average $[H^+]_{in\text{-}situ}$ for samples with low and high in-situ acidity was 20 ± 3 nmol m^{-3} and 113 ± 13 nmol m^{-3}, respectively, while on hazy days, the average $[H^+]_{in\text{-}situ}$ was 28 ± 7 and 182 ± 34 nmol m^{-3} with low and high acidities, respectively. It was found that during non-hazy period, chemical components i.e., OM, SO_4^{2-} and NO_3^- in $PM_{2.5}$ were not affected by the degree of aerosol acidity (t-test, $p > 0.05$) (Fig. 5(a)). Here, we assumed that OM = 2 × OC due to the fact that the sampling site was mainly affected by regional air masses, and previous studies conducted in this region demonstrated the appropriateness of the use of conversion factor of 2.0 [54–56]. In contrast, the mass concentrations of OM and SO_4^{2-} showed significant enhancement with the increase of $[H^+]_{in\text{-}situ}$ in hazy periods (t-test, $p < 0.05$) (Fig. 5(b)). The average difference for OM and SO_4^{2-} between low and high $[H^+]_{in\text{-}situ}$ on hazy days reached 20.1 and 7.3 μg m^{-3}, respectively.

It is worth to explore the reason why the mass concentration of OM increased with the increase of $[H^+]_{in\text{-}situ}$ on hazy days. OC can be simply divided into two groups based on the EC-tracer method, i.e., primary OC (POC) and secondary OC (SOC) [57]. It is noteworthy that the uncertainty of SOC caused by the calculation of OM should be minor because it was based on the ratio of OC/EC. On hazy days, the concentration of POC was 10.5 ± 1.7 μg m^{-3} for the samples with low acidity and 12.2 ± 2.8 μg m^{-3} for the samples with high acidity (t-test, $p > 0.05$), whereas, the concentration of SOC was 9.5 ± 1.5 μg m^{-3} and 17.5 ± 5.8 μg m^{-3} for the two acidities, respectively (t-test, $p < 0.05$). This meant that the increased OC (or OM) with the increase of acidity was largely due to the enhancement of SOC. In other words, high enough $[H^+]_{in\text{-}situ}$ on hazy days was necessary to promote the formation of SOC, which would not occur on non-hazy days due to low $[H^+]_{in\text{-}situ}$. Further inspection indicated that apparent increase of SOC only happened when the $[H^+]_{in\text{-}situ}$ ranged from 85 to 240 nmol m^{-3} on hazy days. The findings are consistent with the study conducted in the Indo-Gangetic Plain in South Asia, in which a significant co-variability was observed between temporal trend of $[H^+]_{total}$ and SOC [25]. The increase of SOC with increased aerosol acidity was also observed in many laboratory studies. Jang et al. [6] discovered that acid-catalyzed heterogeneous reactions of aliphatic aldehydes could increase OM

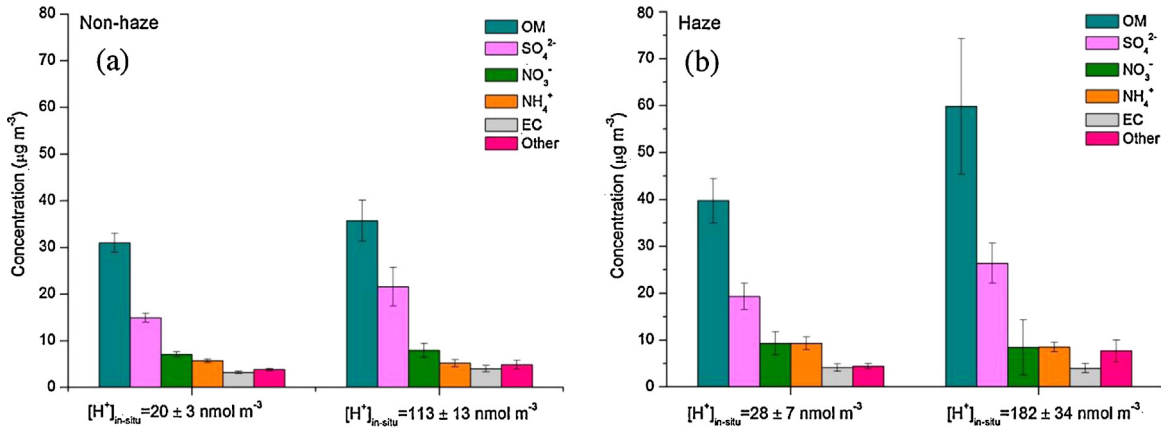

Fig. 5. $PM_{2.5}$ compositions with low and high $[H^+]_{in\text{-}situ}$: (a) in non-hazy period, and (b) in hazy period. "Other" in the figure indicates the summed concentration of Na^+, Cl^-, K^+, Mg^{2+} and Ca^{2+}. Error bars are the 95% confidence interval.

formation by a factor of 5. Surratt et al. [21] found that when $[H^+]_{in\text{-}situ}$ reached 275–517 nmol m^{-3}, OC increased from 20.7 to 31.1 μg m^{-3}. It is noteworthy that particulate SOC formation was a vital reason for the formation of hazy episodes [17,58,59], and large proportion of SOC was developed through acid-catalyzed heterogeneous reaction [6,20,60,61]. Hence, during fall-winter in the PRD region, the acid-catalyzed SOC formation on hazy days could be more significant when aerosol acidity was larger than 83 nmol m^{-3}. Nevertheless, the concentration of SOC did not show any significant correlation with $[H^+]_{in\text{-}situ}$ although the sampling period lasted for 6 years. This was owing to some confounding factors that caused the indistinct link between SOC and $[H^+]_{in\text{-}situ}$, i.e., large proportion of POC, changes of OC/EC ratio, different chemical evolution of precursors and diverse impacts of $[H^+]_{in\text{-}situ}$ on different components of SOC [26]. All these factors would play important roles in the SOA formation in the region. Further study on the influence of acid-catalysis on specific components in SOC is needed.

3.3. Relationship between in-situ acidity and the formation of NO_3^-

The R value in Eq. (1) is an indicator of aerosol acidity. Linear regression analysis between $[NH_4^+]$ and $\{2 \times [SO_4]^{2-} + [NO_3]^-\}$ in all samples found that the slope was 0.66 ($R^2 = 0.76$, F-test, $p < 0.05$), suggesting that NH_4^+ could not be fully neutralized by SO_4^{2-} and NO_3^-. Fig. 6(a) illustrates the logarithmic relationship between R and $[H^+]_{in\text{-}situ}$ ($R^2 = 0.67$, F-test, $p < 0.05$). The R value decreased rapidly from 1.0 to 0.6 when $[H^+]_{in\text{-}situ}$ increased from 0.2 to 83 nmol m^{-3}. However, when $[H^+]_{in\text{-}situ}$ enhanced from 83 to 240 nmol m^{-3}, the R value decreased only from 0.6 to 0.4, implying that the R values of 0.6 and 1 were the thresholds for different acidity of aerosol over the PRD region. Data points with $R \leq 0.6$ corresponded to elevated $[H^+]_{in\text{-}situ}$ values, suggesting high acid content in $PM_{2.5}$. In contrast, $1 > R > 0.6$ meant low acid content of aerosol. Furthermore, if $R > 1$, it indicated that SO_4^{2-} and NO_3^- were completely neutralized, and the excess NH_4^+ caused the particles alkaline.

Basically, there are two major pathways for the formation of particulate nitrate. The first pathway is that nitric acid reacts with ammonia to form NH_4NO_3 in aerosol phase:

$$HNO_{3(g)} + NH_{3(g)} \rightleftarrows NH_4NO_{3(s,aq)} \quad (4)$$

The second formation mechanism is the hydrolysis of N_2O_5, which is the major channel of nitrate formation during nighttime hours [62–66].

$$N_2O_{5(aq)} + H_2O_{(aq)} \rightarrow 2HNO_{3(aq)} \quad (5)$$

In the $H_2SO_4 - HNO_3 - NH_3$ thermodynamic system, the formation of NO_3^- is NH_3-sensitive [4]. NH_3 preferably neutralizes acidic sulfate in more acidic system, and the additional NH_3 is then available to stabilize nitrate [33,40,43,66]. As such, the linear correlation between $[NH_4^+]/[SO_4^{2-}]$ and $[NO_3^-]/[SO_4^{2-}]$ is often used

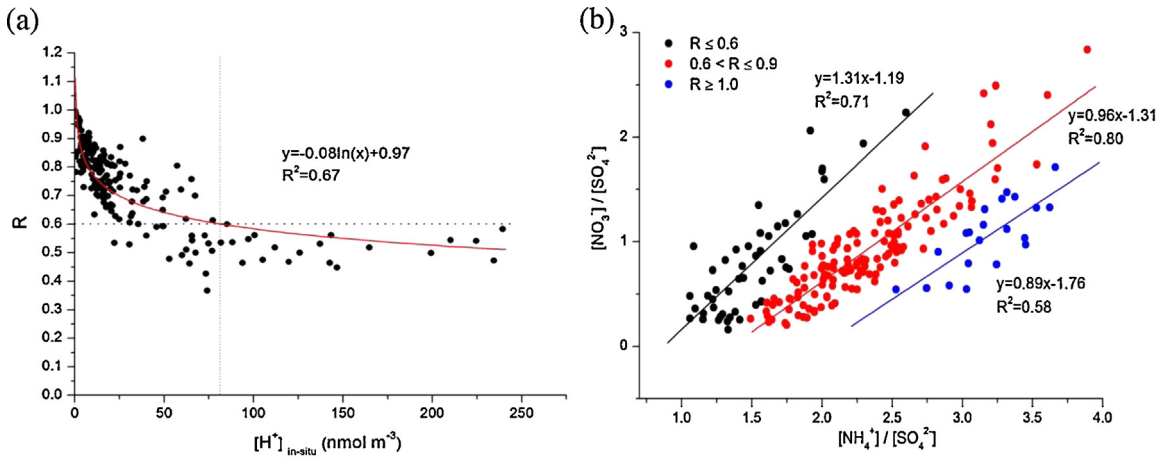

Fig. 6. (a) Logarithmic relationship between R and $[H^+]_{in\text{-}situ}$. (b) Molar ratio of $[NH_4^+]/[SO_4^{2-}]$ versus $[NO_3^-]/[SO_4^{2-}]$ in different ranges of R value; black dot: $R \leq 0.6$; red dot: $0.6 < R \leq 0.9$; blue dot: $R \geq 1.0$. (For interpretation of the references to color in this figure legend, the reader is referred to the web version of this article.)

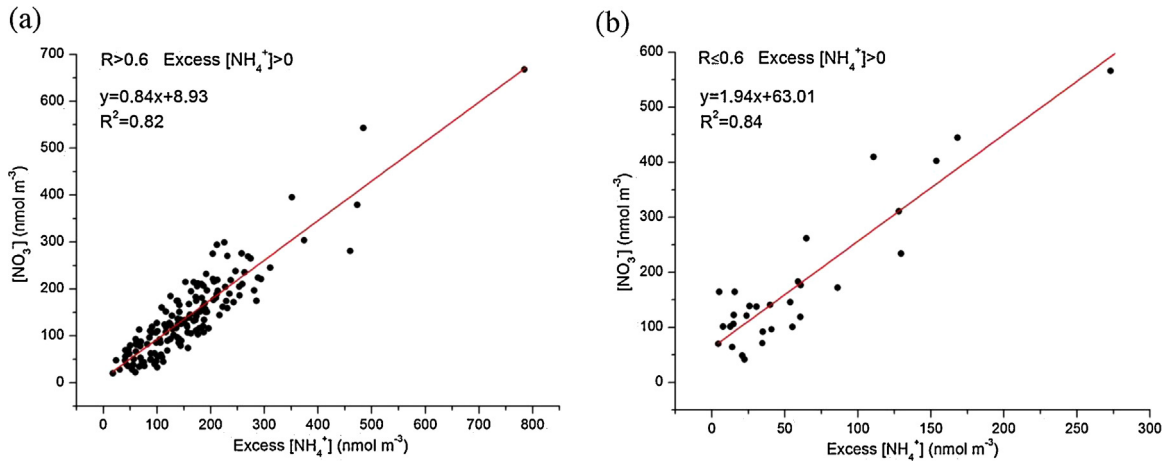

Fig. 7. Linear correlation between $[NO_3^-]$ and excess $[NH_4^+]$: (a) when $R > 0.6$ and excess $[NH_4^+] > 0$, and (b) when $R \leq 0.6$ and excess $[NH_4^+] > 0$.

to explore the formation of NO_3^- in different loadings of SO_4^{2-} [40,41,43,45] (Fig. 6(b)). The data points were divided into 3 groups depending on the R values. Significant linear correlations were found for all the 3 groups (F-test, $p < 0.05$). As the slopes indicated the ratio of $[NO_3^-]$ to $[NH_4^+]$, the slope of 0.96 suggested that NH_4^+ was sufficient to react with almost all of the NO_3^-. Hence, samples with $0.6 < R \leq 0.9$ were chosen to calculate the excess $[NH_4^+]$. Assuming that $[NO_3^-]/[SO_4^{2-}]$ was zero, the intercept of the regression line was 1.36, which was used to calculate the excess $[NH_4^+]$:

$$\text{Excess}[NH_4^+] = ([NH_4^+]/[SO_4^{2-}] - 1.36) \times [SO_4^{2-}] \quad (4)$$

It is noteworthy that though data points with $R \geq 1$ all had high $[NH_4^+]/[SO_4^{2-}]$ ratio (>2) (Fig. 6(b)), these samples were actually alkaline, and all NO_3^- ions had already been neutralized. Hence, these data points would not be used to calculate excess $[NH_4^+]$. The value of 1.36 was the cut-point to distinguish the ammonium-poor (AP′) (i.e., $[NH_4^+]/[SO_4^{2-}] < 1.36$) and ammonium-rich (AR′) (i.e., $[NH_4^+]/[SO_4^{2-}] > 1.36$) samples (to distinguish the definition from previous studies, we used AP′ and AR′).

Unlike previous study [43], high NO_3^- level was not found under the AP′ condition, neither was the relationship between excess $[NH_4^+]$ and $[NO_3^-]$ in the 6-year sampling period (data not shown). In contrast, samples under AR′ condition were divided into two groups according to the R threshold value of 0.6 (Fig. 6(a)). Significant linear correlation was observed between excess $[NH_4^+]$ and $[NO_3^-]$ for both low and high acid content of aerosol (F-test, $p < 0.05$), in line with the observations in AR samples (i.e., $[NH_4^+]/[SO_4^{2-}] > 1.5$) in [41] and [43]. Fig. 7 presents the relationship between excess $[NH_4^+]$ and $[NO_3^-]$. The slope for the samples with $R > 0.6$ was 0.84, close to 1 (Fig. 7(a)), perhaps suggesting the prevalence of homogenous reaction between HNO_3 and NH_3 under the condition of low acidity. On the other hand, for the samples with $R \leq 0.6$, the slope (1.94) was about 2 (Fig. 7(b)). The high $[H^+]_{in\text{-}situ}$ might inhibit the hydrolysis of solid-phase NH_4NO_3 and was likely to further prevent the gas-phase NH_4NO_3 from formation through homogenous reaction partitioning onto the aerosol surface. Consequently, heterogeneous reaction of NO_3^- tended to become significant. Overall, the NO_3^- formation mechanisms in fall-winter of the PRD region had close relationship with in-situ aerosol acidity. When the aerosol acidity was low ($R > 0.6$), NO_3^- was most likely formed through homogenous reaction between HNO_3 and NH_3. In contrast, when the aerosol acidity was high ($R \leq 0.6$), the gas-phase formation of NH_4NO_3 was probably inhibited and the proportion of NO_3^- produced via heterogeneous reaction of N_2O_5 might dominate.

4. Conclusions

In this study, the $PM_{2.5}$ acidity was explored at a background site in the PRD region during fall-winter of 2007–2012. $[H^+]_{total}$ and $[H^+]_{in\text{-}situ}$ significantly reduced ($p < 0.05$) with a rate of -32 ± 1.5 nmol m^{-3} year^{-1} ($R^2 = 0.99$) and -9 ± 1.7 nmol m^{-3} year^{-1} ($R^2 = 0.86$), respectively, attributable to the fact that the decreasing rate of $[H^+]_{total}$ due to the decrease of SO_4^{2-} exceeded the increasing rate caused by the growth of NO_3^- in these years. Obvious difference in $PM_{2.5}$ acidity and LWC concentration was observed between hazy and non-hazy periods. The $[H^+]_{total}$, $[H^+]_{in\text{-}situ}$, $[HSO_4^-]$ and LWC on hazy days were 0.9–2.2, 1.2–3.5, 0.9–2.0 and 2.0–3.0 times than those on non-hazy days, respectively. The large amount of LWC appeared in the hazy periods helped to dissociate more in-situ H^+, which was not caused by the dissociation of HSO_4^-, but by other water-soluble organic/inorganic acids. As an indicator of aerosol acidity, $R = 0.6$ (i.e., $[H^+]_{in\text{-}situ} = 83$ nmol m^{-3}) was the threshold to differentiate the degree of aerosol acidity over the PRD region. On hazy days, the concentrations of OM showed significant increase (t-test, $p < 0.05$) when the acidity increased from low to high ($[H^+]_{in\text{-}situ} > 83$ nmol m^{-3}), which was not observed on non-hazy days. The abundant OC under the condition of high acidity was largely due to the enhancement of SOC. In addition, the NO_3^- formation in fall-winter in the PRD region was closely related to aerosol acidity.

Acknowledgments

This project was supported by the National Natural Science Foundation of China (#41025012 and 41275122), the Strategic Priority Research Program of the Chinese Academy of Sciences (Grant No. XDB05010200), the Hong Kong Research Grants Council (PolyU5154/13E and PolyU152052/14E), the Public Policy Research Scheme of Hong Kong (2013.A6.012.13A), and the Joint Supervision Scheme of the Hong Kong Polytechnic University (G-UB67).

References

[1] J.C. Chow, L.W.A. Chen, J.G. Watson, D.H. Lowenthal, K.A. Magliano, K. Turkiewicz, D.E. Lehrman, $PM_{2.5}$ chemical composition and spatiotemporal variability during the California Regional $PM_{10}/PM_{2.5}$ Air Quality Study (CRPAQS), J. Geophys. Res. -Atmos. 111 (2006) D10S04.
[2] C.K. Chan, X. Yao, Air pollution in mega cities in China, Atmos. Environ. 42 (2008) 1–42.
[3] X. Wang, X. Ding, X. Fu, Q. He, S. Wang, F. Bernard, X. Zhao, D. Wu, Aerosol scattering coefficients and major chemical compositions of fine particles

observed at a rural site hit the central Pearl River Delta, South China, J. Environ. Sci. -China 24 (2012) 72–77.
[4] J.H. Seinfeld, S.M. Pandis, Atmospheric Chemistry and Physics: From Air Pollution to Climate Change, second ed., John Wiley and Sons, New York, 2006.
[5] R.C. Gwynn, R.T. Burnett, G.D. Thurston, A time-series analysis of acidic particulate matter and daily mortality and morbidity in the Buffalo, New York, region, Environ. Health Perspect. 108 (2000) 125–133.
[6] M.S. Jang, N.M. Czoschke, S. Lee, R.M. Kamens, Heterogeneous atmospheric aerosol production by acid-catalyzed particle-phase reactions, Science 298 (2002) 814–817.
[7] J.G. Watson, Visibility: science and regulation, J. Air Waste Manage. Assoc. 52 (2002) 628–713.
[8] J.H. Guo, X.J. Liu, Y. Zhang, J.L. Shen, W.X. Han, W.F. Zhang, P. Christie, K.W.T. Goulding, P.M. Vitousek, F.S. Zhang, Significant acidification in major Chinese croplands, Science 327 (2010) 1008–1010.
[9] A. Khlystov, C.O. Stanier, S. Takahama, S.N. Pandis, Water content of ambient aerosol during the Pittsburgh air quality study, J. Geophys. Res. -Atmos. 110 (2005) D07S10.
[10] Y.F. Cheng, A. Wiedensohler, H. Eichler, H. Su, T. Gnauk, E. Brueggemann, H. Herrmann, J. Heintzenberg, J. Slanina, T. Tuch, M. Hu, Y.H. Zhang, Aerosol optical properties and related chemical apportionment at Xinken in Pearl River Delta of China, Atmos. Environ. 42 (2008) 6351–6372.
[11] H.B. Tan, Y. Yin, X.S. Gu, F. Li, P.W. Chan, H.B. Xu, X.J. Deng, Q.L. Wan, An observational study of the hygroscopic properties of aerosols over the Pearl River Delta region, Atmos. Environ. 77 (2013) 817–826.
[12] I.N. Tang, Chemical and size effects of hygroscopic aerosols on light scattering coefficients, J. Geophys. Res. -Atmos. 101 (1996) 19245–19250.
[13] M. Stock, Y.F. Cheng, W. Birmili, A. Massling, B. Wehner, T. Muller, S. Leinert, N. Kalivitis, N. Mihalopoulos, A. Wiedensohler, Hygroscopic properties of atmospheric aerosol particles over the Eastern Mediterranean: implications for regional direct radiative forcing under clean and polluted conditions, Atmos. Chem. Phys. 11 (2011) 4251–4271.
[14] J. Chen, C.S. Zhao, N. Ma, P.F. Liu, T. Gobel, E. Hallbauer, Z.Z. Deng, L. Ran, W.Y. Xu, Z. Liang, H.J. Liu, P. Yan, X.J. Zhou, A. Wiedensohler, A parameterization of low visibilities for hazy days in the North China Plain, Atmos. Chem. Phys. 12 (2012) 4935–4950.
[15] X. Deng, X. Tie, D. Wu, X. Zhou, X. Bi, H. Tan, F. Li, C. Hang, Long-term trend of visibility and its characterizations in the Pearl River Delta (PRD) region, China, Atmos. Environ. 42 (2008) 1424–1435.
[16] Y.L. Sun, G.S. Zhuang, A.H. Tang, Y. Wang, Z.S. An, Chemical characteristics of $PM_{2.5}$ and PM_{10} in hazy-fog episodes in Beijing, Environ. Sci. Technol. 40 (2006) 3148–3155.
[17] J.H. Tan, J.C. Duan, K.B. He, Y.L. Ma, F.K. Duan, Y. Chen, J.M. Fu, Chemical characteristics of $PM_{2.5}$ during a typical hazy episode in Guangzhou, J. Environ. Sci. -China 21 (2009) 774–781.
[18] G.N. Robinson, D.R. Worsnop, J.T. Jayne, C.E. Kolb, P. Davidovits, Heterogeneous uptake of $ClONO_2$ and N_2O_5 by sulfuric acid solutions, J. Geophys. Res. -Atmos. 102 (1997) 3583–3601.
[19] M. Hallquist, D.J. Stewart, J. Baker, R.A. Cox, Hydrolysis of N_2O_5 on submicron sulfuric acid aerosols, J. Phys. Chem. A 104 (2000) 3984–3990.
[20] S. Gao, N.L. Ng, M. Keywood, V. Varutbangkul, R. Bahreini, A. Nenes, J.W. He, K.Y. Yoo, J.L. Beauchamp, R.P. Hodyss, R.C. Flagan, J.H. Seinfeld, Particle phase acidity and oligomer formation in secondary organic aerosol, Environ. Sci. Technol. 38 (2004) 6582–6589.
[21] J.D. Surratt, M. Lewandowski, J.H. Offenberg, M. Jaoui, T.E. Kleindienst, E.O. Edney, J.H. Seinfeld, Effect of acidity on secondary organic aerosol formation from isoprene, Environ. Sci. Technol. 41 (2007) 5363–5369.
[22] Q. Zhang, J.L. Jimenez, D.R. Worsnop, M. Canagaratna, A case study of urban particle acidity and its influence on secondary organic aerosol, Environ. Sci. Technol. 41 (2007) 3213–3219.
[23] R.L. Tanner, K.J. Olszyna, E.S. Edgerton, E. Knipping, S.L. Shaw, Searching for evidence of acid-catalyzed enhancement of secondary organic aerosol formation using ambient aerosol data, Atmos. Environ. 43 (2009) 3440–3444.
[24] R. Rengarajan, A.K. Sudheer, M.M. Sarin, Aerosol acidity and secondary organic aerosol formation during wintertime over urban environment in western India, Atmos. Environ. 45 (2011) 1940–1945.
[25] B. Srinivas, M.M. Sarin, $PM_{2.5}$, EC and OC in atmospheric outflow from the Indo-Gangetic Plain: temporal variability and aerosol organic carbon-to-organic mass conversion factor, Sci. Total Environ. 487 (2014) 196–205.
[26] S. Takahama, C.I. Davidson, S.N. Pandis, Semicontinuous measurements of organic carbon and acidity during the Pittsburgh air quality study: implications for acid-catalyzed organic aerosol formation, Environ. Sci. Technol. 40 (2006) 2191–2199.
[27] USEPA, Determination of the Strong Acidity of Atmospheric Fine-particles(<2.5 μm), Compendium Method IO-4.1, EPA/625/R-96/010a, 1999.
[28] R.A. Stairs, J. Semmler, Estimation of acidity in rainfall by electrical-conductivity, Anal. Chem. 57 (1985) 740–743.
[29] K. Ito, C.C. Chasteen, H.K. Chung, S.K. Poruthoor, G.F. Zhang, P.K. Dasgupta, A continuous monitoring system for strong acidity in aerosols, Anal. Chem. 70 (1998) 2839–2847.
[30] X.H. Yao, M. Fang, C.K. Chan, K.F. Ho, S.C. Lee, Characterization of dicarboxylic acids in $PM_{2.5}$ in Hong Kong, Atmos. Environ. 38 (2004) 963–970.
[31] X.F. Huang, M. Hu, L.Y. He, X.Y. Tang, Chemical characterization of water-soluble organic acids in $PM_{2.5}$ in Beijing, China, Atmos. Environ. 39 (2005) 2819–2827.
[32] M. Hu, Z.J. Wu, J. Slanina, P. Lin, S. Liu, L.M. Zeng, Acidic gases ammonia and water-soluble ions in $PM_{2.5}$ at a coastal site in the Pearl River Delta, China, Atmos. Environ. 42 (2008) 6310–6320.
[33] R.K. Pathak, X.H. Yao, C.K. Chan, Sampling artifacts of acidity and ionic species in $PM_{2.5}$, Environ. Sci. Technol. 38 (2004) 254–259.
[34] X.H. Yao, T.Y. Ling, M. Fang, C.K. Chan, Comparison of thermodynamic predictions for in-situ pH in $PM_{2.5}$, Atmos. Environ. 40 (2006) 2835–2844.
[35] Y. Zhou, L.K. Xue, T. Wang, X.M. Gao, Z. Wang, X.F. Wang, J.M. Zhang, Q.Z. Zhang, W.X. Wang, Characterization of aerosol acidity at a high mountain site in central eastern China, Atmos. Environ. 51 (2012) 11–20.
[36] P. Saxena, A.B. Hudischewskyj, C. Seigneur, J.H. Seinfeld, A comparative-study of equilibrium approaches to the chemical characterization of secondary aerosols, Atmos. Environ. 20 (1986) 1471–1483.
[37] Z.Y. Meng, J.H. Seinfeld, On the source of the submicrometer droplet mode of urban and regional aerosols, Aerosol Sci. Technol. 20 (1994) 253–265.
[38] A. Nenes, S.N. Pandis, C. Pilinis, ISORROPIA: a new thermodynamic equilibrium model for multiphase multicomponent inorganic aerosols, Aquat. Geochem. 4 (1998) 123–152.
[39] S.L. Clegg, P. Brimblecombe, A.S. Wexler, Thermodynamic model of the system H^+–NH_4^+–SO_4^{2-}–NO_3^-–H_2O at tropospheric temperatures, J. Phys. Chem. A 102 (1998) 2137–2154.
[40] R.K. Pathak, P.K.K. Louie, C.K. Chan, Characteristics of aerosol acidity in Hong Kong, Atmos. Environ. 38 (2004) 2965–2974.
[41] K. He, Q. Zhao, Y. Ma, F. Duan, F. Yang, Z. Shi, G. Chen, Spatial and seasonal variability of $PM_{2.5}$ acidity at two Chinese megacities: insights into the formation of secondary inorganic aerosols, Atmos. Chem. Phys. 12 (2012) 1377–1395.
[42] R.K. Pathak, X.H. Yao, A.K.H. Lau, C.K. Chan, Acidity and concentrations of ionic species of $PM_{2.5}$ in Hong Kong, Atmos. Environ. 37 (2003) 1113–1124.
[43] R.K. Pathak, W.S. Wu, T. Wang, Summertime $PM_{2.5}$ ionic species in four major cities of China: nitrate formation in an ammonia-deficient atmosphere, Atmos. Chem. Phys. 9 (2009) 1711–1722.
[44] S.H. Cheng, L.X. Yang, X.H. Zhou, L.K. Xue, X.M. Gao, Y. Zhou, W.X. Wang, Size-fractionated water-soluble ions, situ pH and water content in aerosol on hazy days and the influences on visibility impairment in Jinan, China, Atmos. Environ. 45 (2011) 4631–4640.
[45] X. Huang, R. Qiu, C.K. Chan, P.R. Kant, Evidence of high $PM_{2.5}$ strong acidity in ammonia-rich atmosphere of Guangzhou, China: transition in pathways of ambient ammonia to form aerosol ammonium at $[NH_4^+]/[SO_4^{2-}] = 1.5$, Atmos. Res. 99 (2011) 488–495.
[46] J. Xue, A.K.H. Lau, J.Z. Yu, A study of acidity on $PM_{2.5}$ in Hong Kong using online ionic chemical composition measurements, Atmos. Environ. 45 (2011) 7081–7088.
[47] X.X. Fu, X.M. Wang, H. Guo, K. Cheung, X. Ding, X.Y. Zhao, Q.F. He, B. Gao, Z. Zhang, T.Y. Liu, Y.L. Zhang, Trends of ambient fine particles and major chemical components in the Pearl River Delta region: observation at a regional background site in fall and winter, Sci. Total Environ. 497–498 (2014) 274–281.
[48] Y.H. Ding, J.C.L. Chan, The East Asian summer monsoon: an overview, Meteorol. Atmos. Phys. 89 (2005) 117–142.
[49] S.J. Fan, B.M. Wang, M. Tesche, R. Engelmann, A. Althausen, J. Liu, W. Zhu, Q. Fan, M.H. Li, N. Ta, L.L. Song, K.C. Leong, Meteorological conditions and structures of atmospheric boundary layer in October 2004 over Pearl River Delta area, Atmos. Environ. 42 (2008) 6174–6186.
[50] S. Liu, M. Hu, S. Slanina, L.Y. He, Y.W. Niu, E. Bruegemann, T. Gnauk, H. Herrmann, Size distribution and source analysis of ionic compositions of aerosols in polluted periods at Xinken in Pearl River Delta (PRD) of China, Atmos. Environ. 42 (2008) 6284–6295.
[51] NIOSH, Method 5040 Issue 3 (Interim): elemental carbon (diesel exhaust), in: NIOSH Manual of Analytical Methods, fourth ed., National Institute of Occupational Safety and Health, Cincinnati, OH, 1999.
[52] I.N. Tang, H.R. Munkelwitz, Water activities,densities, and refractive-indexes of aqueous sulfates and sodium-nitrate droplets of atmospheric improtance, J. Geophys. Res. -Atmos. 99 (1994) 18801–18808.
[53] Y.X. Bian, C.S. Zhao, N. Ma, J. Chen, W.Y. Xu, A study of aerosol liquid water content based on hygroscopicity measurements at high relative humidity in the North China Plain, Atmos. Chem. Phys. 14 (2014) 6417–6426.
[54] X. Chen, J.Z. Yu, Measurement of organic mass to organic carbon ratio in ambient aerosol samples using a gravimetric technique in combination with chemical analysis, Atmos. Environ. 41 (2007) 8857–8864.
[55] M.O. Andreae, O. Schmid, H. Yang, D.L. Chand, J.Z. Yu, L.M. Zeng, Y.H. Zhang, Optical properties and chemical composition of the atmospheric aerosol in urban Guangzhou, China, Atmos. Environ. 42 (2008) 6335–6350.
[56] L. Xing, T.M. Fu, J.J. Cao, S.C. Lee, G.H. Wang, K.F. Ho, M.C. Cheng, C.F. You, T.J. Wang, Seasonal and spatial variability of the OM/OC mass ratios and high regional correlation between oxalic acid and zinc in Chinese urban organic aerosol, Atmos. Chem. Phys. 13 (2013) 4307–4318.
[57] B.J. Turpin, J.J. Huntzicker, Identification of secondary organic aerosol episodes and quantitation of primary and secondary organic aerosol concentrations during scaqs, Atmos. Environ. 29 (1995) 3527–3544.
[58] B. Hou, G. Zhuang, R. Zhang, T. Liu, Z. Guo, Y. Chen, The implication of carbonaceous aerosol to the formation of hazy: revealed from the

characteristics and sources of OC/EC over a mega-city in China, J. Hazard. Mater. 190 (2011) 529–536.
[59] D.S. Ji, L. Li, Y.S. Wang, J.K. Zhang, M.T. Cheng, Y. Sun, Z.R. Liu, L.L. Wang, G.Q. Tang, B. Hu, N. Chao, T.X. Wen, H.Y. Miao, The heaviest particulate air-pollution episodes occurred in northern China in January, 2013: insights gained from observation, Atmos. Environ. 92 (2014) 546–556.
[60] M.S. Jang, B. Carroll, B. Chandramouli, R.M. Kamens, Particle growth by acid-catalyzed heterogeneous reactions of organic carbonyls on preexisting aerosols, Environ. Sci. Technol. 37 (2003) 3828–3837.
[61] A. Limbeck, M. Kulmala, H. Puxbaum, Secondary organic aerosol formation in the atmosphere via heterogeneous reaction of gaseous isoprene on acidic particles, Geophys. Res. Lett. 30 (2003), http://dx.doi.org/10.1029/2003GL017738.
[62] M. Moya, A.S. Ansari, S.N. Pandis, Partitioning of nitrate and ammonium between the gas and particulate phases during the 1997 IMADA-AVER study in Mexico City, Atmos. Environ. 35 (2001) 1791–1804.
[63] X. Wang, Y. Zhang, H. Chen, X. Yang, J. Chen, F. Geng, Particulate nitrate formation in a highly polluted urban area: a case study by single-particle mass spectrometry in Shanghai, Environ. Sci. Technol. 43 (2009) 3061–3066.
[64] W.L. Chang, P.V. Bhave, S.S. Brown, N. Riemer, J. Stutz, D. Dabdub, Heterogeneous atmospheric chemistry, ambient measurements, and model calculations of N_2O_5: a review, Aerosol Sci. Technol. 45 (2011) 665–695.
[65] J. Xue, Z.B. Yuan, A.K.H. Lau, J.Z. Yu, Insights into factors affecting nitrate in $PM_{2.5}$ in a polluted high NOx environment through hourly observations and size distribution measurements, J. Geophys. Res. -Atmos. 119 (2014) 4888–4902.
[66] A.S. Ansari, S.N. Pandis, Response of inorganic PM to precursor concentrations, Environ. Sci. Technol. 32 (1998) 2706–2714.